

EFFECT OF ROUGHNESS GEOMETRY ON CHARACTERISTICS OF PHASE CHANGE MATERIAL STORAGE UNIT FOR NIGHT COOLNESS STORAGE IN SUMMER SEASON

by

Shailendra Kumar SHUKLA* and Satish K. SINGH

Mechanical Engineering Department, Indian Institute of Technology (BHU), Varanasi, India

Original scientific paper

DOI: 10.2298/TSCI110511023S

This paper presents a theoretical analysis of thermal storage unit using phase change material as storage medium. Storage unit consists of parallel rectangular channels for the air flow which are separated by phase change storage material. The purpose of storage unit is to absorb the night coolness and to provide cooled air at comfort temperature during day time in summer season. MATLAB simulation tool has been used to compute the air temperature variation with location as well as time, charging, and discharging time of storage unit. Phase change material used for analysis is selected in such a way that its melting point lies between comfort temperature and minimum night ambient temperatures. The air flow rate needed for charging of phase change material is approximately four times greater than the flow rate required during day time to achieve comfort temperature for approximately eight hours, due to limited summer night time (only eight hours). The length of storage unit for which number transfer of units value is greater than or equal to five will give the exit air temperature equal to phase change material temperature for the case of latent heat utilization. It is found that artificial roughness on the duct surface effectively reduces the length of storage unit in the cost of some extra pressure drop across the duct.

Key words: *phase change material, storage unit, air temperature, comfort temperature, number transfer of units, night coolness, artificial roughness*

Introduction

Energy storage not only plays an important role in conservation of the energy but also improves the performance and reliability of wide range of energy systems, and become more important where the energy sources are intermittent. Due to the increased environmental concerns and limited nature of fossil fuels passive ways of space conditioning are getting more attention like solar cooling/heating, storage of night coolness, earth coupled cooling/heating systems, phase change material (PCM) based cooling/heating systems, etc. Since many of the resources on which passive techniques depend are intermittent in nature so storage of these resources always plays a vital role for continuous utilization of these resources. So an efficient and reliable thermal energy storage system plays a vital role when talking about passive techniques. Thermal energy storage can be in form of sensible heat of liquid or solid, storage of high pressure steam, heat of hydration or utilization of heat of fusion or heat of evaporation. Among all above mentioned storage techniques latent heat storage energy technique is getting more attraction due to their very high energy storage densities and smaller temperature difference when storing the en-

* Corresponding author; e-mail: skshukla.mec@itbhu.ac.in

ergy and releasing it as compare to sensible storage technique. Using coolness of night to achieve comfort temperatures in a space is one of the passive ways of cooling. If this night coolness is stored and being used during day time to achieve the comfort temperatures mechanical cooling can be either totally eliminated from day time also or at least can be limited to certain period of day time. Same can be practiced during winters, if in winter solar energy during day time is stored and used for night time heating a large amount of fossil fuels can be left unburnt which may help in reduction of pollutant gases like NO_x and CO_2 . In this paper the study of PCM storage unit for night coolness storage system has been done with an objective to reduce the length of storage system by using different artificial roughness geometry which in turn reduces the cost of its use.

Literature survey

Hed and Bellander [1] presented a method to simulate a PCM air heat exchanger. PCM used is having phase change in a given temperature range. The aim was to find a model that will fit into a finite difference based indoor climate and energy simulation software. To do that a fictive heat transfer coefficient is established. The fictive heat transfer coefficient includes aspects of the geometry and the airflow in the heat exchanger as well as the material properties of the PCM.

Alkilani *et al.*, [2] presented theoretical investigation of output air temperatures due to a discharge process in a solar air heater integrated with a PCM. PCM unit consist of inline single row of cylinders containing PCM. The PCM consists of paraffin wax with mass fraction 0.5% aluminum powder to enhance the heat transfer.

Stritih and Butala [3] presented the experimental and numerical analysis of cooling buildings using night-time cold accumulation in PCM with constant inlet temperatures. The comparison of experimental and numerical results shows good agreement.

Arkar and Medved [4] have presented a numerical study the free cooling concept with varying inlet temperatures using RT 20 paraffin as PCM which is integrated into the ventilation system of the building. The cylindrical latent heat thermal energy storage (LHTES) device was filled with spheres of encapsulated RT20 paraffin. In this research a parametric study of storage unit has been carried out and ambient air is being used as inlet air.

The correlation between the climatic conditions and the free cooling potential was investigated by Medved and Arkar [5] for different cities of Europe and for the case of a cylindrical LHTES with a packed bed of spheres encapsulated with PCM that is integrated into a building's mechanical ventilation system. For an experimental verification of the LHTES numerical model a commercially available PCM (RT20 paraffin, Rubitherm GmbH) with a latent heat of 142 kJ/kg was used. This PCM has a relatively large phase change temperature range.

Morison and Abdel-Khalik [6] developed a theoretical model for studying the transient behavior of phase-change energy storage (PCES) unit and studied the performance of solar heating systems using both air and liquid as working fluid, this model based on three assumptions: axial conduction in the flow mode is negligible, Biot number is very low that temperature variations normal to the flow can be neglected, and heat loss from the unit can be ignored.

Solomon [7] studied the behaviour of an array of PCM cylinders as a thermal storage unit under some assumptions which can make this study by looking at a single row of N cylinders. The heat transfer process in every cylinder is radially symmetric, and recommended to use this method to design the systems and their simulation, which is used by the authors in this study to predict the air temperature and freezing time.

Virgone *et al.* [8] performed the assessment of PCM wallboard usage for the renovation of a tertiary (*i. e.* light weight) building. For this purpose, two identical rooms of a renovated tertiary building have been tested, one equipped with PCM wallboard the other being “classically” renovated. The results show that the PCM wallboards enhance the thermal comfort of occupants due to air temperature and radiative effects of the walls.

Susman *et al.* [9], constructed PCM modules from a paraffin composite and tested in an occupied London office, in summer season. Design variations tested the effect on heat transfer of a black paint or aluminum surface, the effect of different phase transition zones and the effect of discharging heat inside or outside. The modules temperatures were monitored along with airflow rate, air temperature and globe temperature. Black modules transfer heat and exhaust latent storage capacity significantly quicker than aluminum modules, due to radiant exchange.

This analysis presents the affect of limited summer night times and temperature during the storage of night coolness using PCM in harsh summer climatic conditions for the utilization of during day time to achieve comfort temperatures from storage outlet. For this purpose storage unit used is composed of multiple rectangular channels for the flow of heat transfer fluid, which is air in this case, separated by the phase change storage material. MATLAB simulation tool has been used to compute the air temperature variation with location as well as time, charging and discharging time of storage unit. Effect of PCM mass, air flow rate and different inlet temperatures are considered both for the day time and night time operation of the storage unit. Melting point of PCM used for analysis is selected in such a way that between comfort temperature and minimum night ambient temperatures. The five artificial roughness geometries on the duct surface as per the order of ability to create turbulence and a smooth surface have been selected. The correlations for heat transfer coefficient and coefficient of friction developed by respective investigators have been used to calculate the required length of storage unit and extra pressure drop across the duct.

Methodology

For the analysis of storage of night coolness using phase change materials storage unit configuration is displayed as in fig. 1. This system consists of two essential parts, PCM channels and air flowing duct in alternate orders. Number of air channels is taken as fives. Dimension of the air flowing duct is $l \times a \times b$ in which l is the length of storage unit, b – the width of storage unit which is taken as 0.45 m, and a – the air gap which depends on air flow rate.

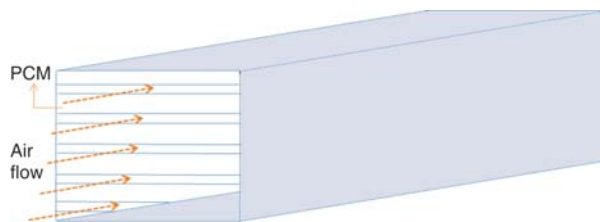


Figure 1. Thermal energy storage unit to be analyzed for night coolness storage

Simplicity of this type of storage unit is the main advantage of its selection. Such types of model have been studied by Morrison and Abdel-Khalik [6] for the thermal energy storage coupled with solar water heating system. Here in this work this type of system is used to be studied with night coolness storage for day time utilization for cooling during summer season.

PCM container and air gap that will be used for the analysis are given in fig. 2. Half thickness of the plate and, respectively, half of its air gap is considered here and other portion of plate with the same thickness and same air gap will behave in the similar way.

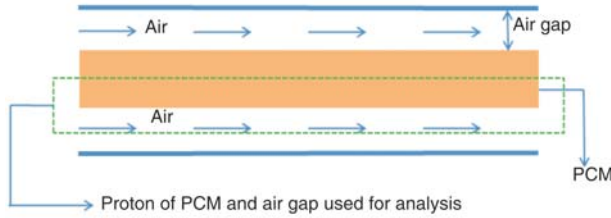


Figure 2. Cross-section of PCM and air gap used for analysis

Analysis is based on the following assumptions:

- material changes phase at a constant temperature,
- properties of PCM in both phases are considered to be constant,
- conduction resistance of material used between PCM and heat transfer fluid is negligible,
- sub cooling of PCM is ignored,
- heat loss from the unit is ignored,
- axial conduction in the flow direction is negligible,
- temperature of PCM is constant with location but it can vary with time [2], and
- air flow in the channel is fully developed.

Governing equation for air as heat transfer fluid is:

$$\dot{m}_a C_{p,a} dT_a = h_a b dx (T_{pcm} - T_a) \quad (1)$$

where

$$\dot{m}_a = \frac{\dot{V}_a \rho_a}{3600} \quad \text{and} \quad \dot{V}_a = u_a A_c$$

Equation (1) can be written with finite difference method in the form:

$$T_{i,a}^n = T_{i-1,a}^n + \frac{h_a b dx (T_{pcm}^n - T_{i-1,a}^n)}{\dot{m}_a C_{p,a}}$$

For fully developed laminar flow in a smooth duct [10], $Re < 2300$

$$Nu = 5.9, \text{ for } b/a = 180 \text{ and } 5.7 \text{ for } b/a = 90$$

For fully developed turbulent flow in a smooth duct [11], $Re > 2300$:

$$Nu = 0.023 Re^{0.8} Pr^{0.3} \text{ for cooling, and } Nu = 0.023 Re^{0.8} Pr^{0.4} \text{ for heating where } f = 0.079 Re^{-0.25}.$$

Heat carried away by air in time interval of Δt at any time:

$$Q = \dot{m}_a C_{p,a} (T_{out}^n - T_{in}^n) \Delta t \quad (2)$$

if there is no phase change $T_{pcm}^{n+1} = T_{pcm}^n + Q/M_{pcm} C_{p,pcm}$ and if there is phase change $T_{pcm} = T_m$.

Following is the relation that has been developed for calculating indoor comfort temperatures for any region which is coupled with mean outdoor temperatures and it is given by Nicol and Raja *et al.* [13]:

$$T_{ic} = 18.5 + 0.36 T_{mo}, \quad T_{mo} = \frac{T_{max} + T_{min}}{2}$$

where, T_{mo} is the mean daily temperature and T_{ic} – the indoor comfort temperature. Comfort temperature range may vary about $\pm 2^\circ C$ for air conditioned space. To overcome the low thermal conductivity problem of PCM we can add a powder of material having good conductivity such as copper or aluminum powder, in goal to low the system cost we preferred aluminum powder (1.5%), the physical properties of the stimulated compound calculated as follows, tab. 1 [2]:

$$k_{eff} = k_{pcm} v_{pcm} + k_{Al} v_{Al}, \quad C_{p,eff} = C_{p,pcm} m_{pcm} + C_{p,Al} m_{Al}, \quad \text{and} \quad \rho_{eff} = \rho_{pcm} v_{pcm} + \rho_{Al} v_{Al}$$

where $v_{pcm} = V_{pcm}/V_{eff}$ is volume fraction of PCM in the compound, $v_{Al} = V_{Al}/V_{eff}$ – the volume fraction of aluminum powder in the compound, $m_{pcm} = M_{pcm}/M_{eff}$ – the mass fraction of PCM in

the compound, $m_{Al} = M_{Al}/M_{eff}$ – the mass fraction of aluminum in the compound. The compound formed after mixing is used as PCM for night coolness storage.

Table 1. Physical properties

Name of Property	SP 25 A8 (PCM)/Rubitherm	Aluminum	Compound
Melting point, (T_m)	27 °C	–	27 °C
Latent heat enthalpy, (L)	180 kJ/kg	–	180 kJ/kg
Density, (ρ)	1380 kg/m ³	2702 kg/m ³	1390 kg/m ³
Thermal conductivity, (k)	0.6 W/mK	237 W/mK	2.45 W/mK
Specific heat, (C_p)	2.5 kJ/kgK	0.896 kJ/kgK	2.47 kJ/kgK

Effect of roughness geometry on heat transfer and friction characteristics

Use of artificial roughness in the form of ribs on the heat transfer plate has been found to be an efficient method of enhancing the performance and to reduce the size of the system. There are several parameters that characterize the roughness elements, but for heat-exchanger the most preferred roughness geometry is repeated rib type, which is described by the dimensionless parameters viz. relative roughness height e/D_h and relative roughness pitch P/e , fig. 3. The friction factor and Nu are function of these dimensionless parameters, assuming that the rib thickness is small relative to rib spacing or pitch. Although the repeated rib surface is considered as roughness geometry, it may also be viewed as a problem in boundary layer separation and re-attachment. The rib creates turbulence, by generating the flow separation regions (vortices) one on each side of the rib, which results in enhancement in heat transfer as well as friction.

Figure 4 shows the various possible flow patterns downstream from a rib, as a function of the relative roughness pitch and relative roughness height. Flow separates at the rib, forms a widening free shear layer, and reattaches at a distance of 6-8 times rib-roughness height downstream from the rib. Re-attachment does not occur for P/e less than about eight except for chamfered rib or rib-groove roughness. The local heat transfer coefficients in the separated flow region are larger than those of an undisturbed boundary layer and wall shear stress is zero at the re-attachment point; the maximum heat transfer occurs in the vicinity of the re-attachment point. A reverse flow boundary layer originates at the re-attachment point and tends toward re-

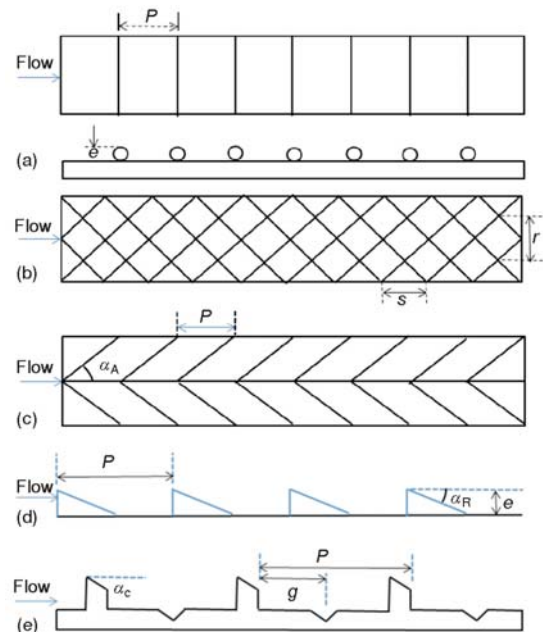


Figure 3. Different types of roughness geometry; (a) circular ribs, (b) expanded metal mesh, (c) V shaped ribs, (d) wedge shaped ribs, (e) chamfered rib-groove

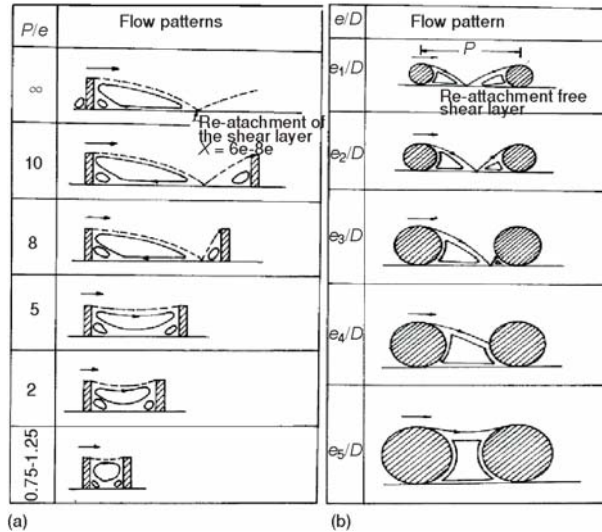


Figure 4. (a) Flow pattern downstream the roughness as a function of relative roughness pitch; (b) Flow patterns downstream the roughness as a function of relative roughness height ($e_5 > e_4 > e_3 > e_2 > e_1$; $P = \text{constant}$) [14]

noticeable increase in heat transfer and moderate fluid Δp could be served.

The optimum chamfering angle on the basis of thermodynamically performance has been reported equal to $15-18^\circ$ [19]. The optimum relative groove position g/P is about 0.4. The induced form drag is reduced due to change in angle of attack for ribs from 90° (transverse), and a better thermal to hydraulic performance is obtained by having optimum angle of attack. As the angle of attack decreases, the friction factor reduces rapidly; however, there is marginal decrease in Nusselt number with change in angle of attack from 90° to 45° .

Results and discussion

Results obtained from the MATLAB computer programs are presented here to show the effect of different parameters during charging and discharging of PCM storage unit. Thermal conductivity of PCM is increased by mixing aluminum powder to reduce Biot number below 0.1 for PCM container. The main aim of this work is to obtain comfort temperature from the storage unit when it is hot in day-time during summer season by utilizing night coolness with air as the

heat transfer fluid. Figure 5 shows the maximum, minimum and comfort temperatures for the location Varanasi, India. The comfort temperature as calculated from the mentioned relation and known climatic data for the month of June is $30 \pm 2^\circ\text{C}$.

Variation of air flow rates, length of storage unit and its effect on air outlet temperature is shown in fig. 6 for inlet air temperature of 40°C . Eight air flow rates have been considered here which varies from $10 \text{ m}^3/\text{h}$ to $80 \text{ m}^3/\text{h}$ with the increment of $10 \text{ m}^3/\text{h}$. All the flow rates

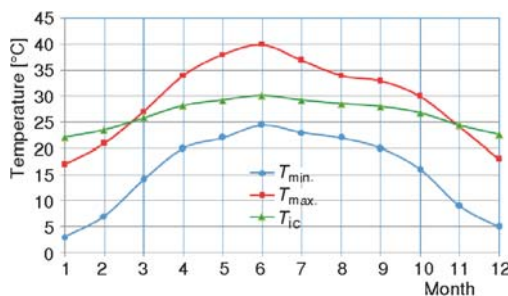


Figure 5. Climatic data for the location Varanasi

Table 2. Correlations for heat transfer and coefficient of friction for various types of artificial roughness

Types of roughness	Nusselt number	Coefficient of friction	Range of parameters
Expanded metal mesh [15]	$\text{Nu} = 4.0 \cdot 10^{-4} (\text{Re})^{1.22} \left(\frac{e}{D_h} \right)^{0.625} \left(\frac{s}{10e} \right)^{2.22} \left(\frac{r}{10e} \right)^{2.22} \cdot \exp \left[-1.25 \left(\ln \frac{s}{10e} \right)^2 \right] \exp \left[-1.25 \left(\ln \frac{r}{10e} \right)^2 \right]$	$f = 0.815 (\text{Re})^{-0.361} \left(\frac{10e}{D_h} \right)^{0.591} \left(\frac{r}{e} \right)^{0.266} \left(\frac{s}{10e} \right)^{-0.19}$	$e/D_h: 0.012-0.039$ $r/e: 25.0-71.78$ $s/e: 15.6-46.87$ $\text{Re}: 1900-13.000$
Circular ribs [14]	$\text{Nu} = 0.08596 (\text{Re})^{0.723} \left(\frac{e}{D_h} \right)^{0.072} \left(\frac{P}{e} \right)^{-0.054} \quad \text{for } e^+ \leq 24$ $\text{Nu} = 0.02954 (\text{Re})^{0.802} \left(\frac{e}{D_h} \right)^{0.021} \left(\frac{P}{e} \right)^{-0.016} \quad \text{for } e^+ > 24$ $e^+ = \frac{e}{D_h} \sqrt{\frac{f}{2}} \text{Re}$	$f = 0.245 (\text{Re})^{-1.25} \left(\frac{e}{D_h} \right)^{0.243} \left(\frac{P}{e} \right)^{-0.206}$	$e/D_h: 0.01-0.03$ $P/e: 10.0-40.0$ $\text{Re}: 5000-20.000$ $e^+: 8.0-42.0$
V shaped ribs [16]	$\text{Nu} = 0.067 (\text{Re})^{0.888} \left(\frac{e}{D_h} \right)^{0.424} \left(\frac{\alpha_A}{60} \right)^{-0.077} \cdot \exp \left[-0.782 \left(\ln \frac{\alpha_A}{60} \right)^2 \right]$	$f = 6.266 (\text{Re})^{-0.425} \left(\frac{e}{D_h} \right)^{0.565} \left(\frac{\alpha_A}{60} \right)^{-0.093} \cdot \exp \left[-0.719 \left(\ln \frac{\alpha_A}{60} \right)^2 \right]$	$e/D_h: 0.02-0.034$ $P/e: 10.0$ $\alpha_A: 30-90^\circ$ $\text{Re}: 2500-18.000$
Wedge shaped ribs [17]	$\text{Nu} = 1.89 \cdot 10^{-4} (\text{Re})^{1.21} \left(\frac{e}{D_h} \right)^{0.426} \left(\frac{P}{e} \right)^{2.94} \left(\frac{\alpha_R}{10} \right)^{-0.018} \cdot \exp \left[-0.71 \left(\ln \frac{P}{e} \right)^2 \right] \exp \left[-1.5 \left(\ln \frac{\alpha_R}{10} \right)^2 \right]$	$f = 12.44 (\text{Re})^{-0.18} \left(\frac{e}{D_h} \right)^{0.99} \left(\frac{P}{e} \right)^{-0.52} \left(\frac{\alpha_R}{10} \right)^{0.49}$	$e/D_h: 0.015-0.033$ $P/e: <12.12$ $P/e: >60.17 \alpha_R^{-1.0264}$ $\alpha_R: 8-15^\circ$ $\text{Re}: 3000-18.000$
Chamfered rib-groove [18]	$\text{Nu} = 0.00225 (\text{Re})^{0.92} \left(\frac{e}{D_h} \right)^{0.52} \left(\frac{P}{e} \right)^{1.72} \left(\frac{g}{P} \right)^{-1.21} \alpha_C^{1.24} \cdot \exp \left[-0.46 \left(\ln \frac{P}{e} \right)^2 \right] \exp \left[-0.22 (\ln \alpha_C)^2 \right] \exp \left[-0.74 \left(\ln \frac{g}{P} \right)^2 \right]$	$f = 0.0024 \cdot 5 (\text{Re})^{-0.124} \left(\frac{e}{D_h} \right)^{0.365} \left(\frac{P}{e} \right)^{-4.32} \left(\frac{g}{P} \right)^{-1.24} \cdot \exp \left[-0.005 \alpha_C \right] \exp \left[-1.09 \left(\ln \frac{P}{e} \right)^2 \right] \exp \left[-0.68 \left(\ln \frac{g}{P} \right)^2 \right]$	$e/D_h: 0.022-0.04$ $P/e: 4.5-10.0$ $g/P: 0.3-0.6$ $\alpha_C: 5-30^\circ$ $\text{Re}: 3000-21.000$

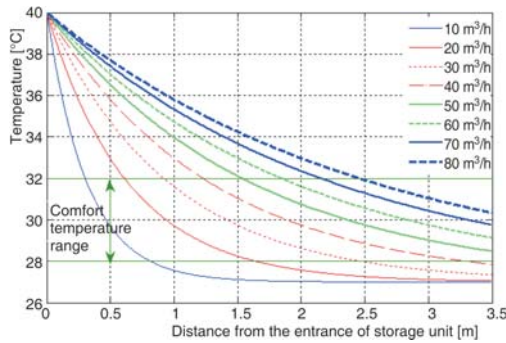


Figure 6. Outlet air temperature vs. length of storage unit during day time operation, $T_{in} = 38\text{ }^{\circ}\text{C}$

required will also generate fully developed flow within 10% length of the minimum length required of the storage unit to obtain comfort temperature. If we select air gap constant and make air velocity variable then either flow will not be fully developed (at lower air flow rate) or the power required for fan will be high (at higher air flow rates). The outlet air temperature is decreasing exponentially with increasing the length of storage unit. The outlet air temperature for higher air flow rate is higher than lower air flow rate at any length of storage unit. At lowest flow rate which is $10\text{ m}^3/\text{h}$, the length of storage unit required is less than 1 meter. The minimum length of storage unit required for the highest flow rate is 3.7 meters.

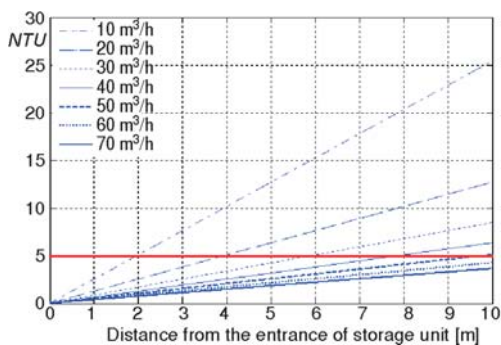


Figure 7. Effect of flow rates and length of storage unit on NTU

temperature limits at the exit of storage unit. On the other hand limitations of space availability and cost are always associated with length of the storage unit. Best approach will be first choose the minimum length in such a way which provides comfort temperature at the start of operation at required flow rate and then use the mass option of PCM to keep the exit air temperature in comfort range for desired time period.

Figure 8 and shows the effect of mass of PCM on discharge time for different inlet air it is assumed that initially PCM is in solid form at its melting point of $27\text{ }^{\circ}\text{C}$. During the melting of PCM its temperature will be constant therefore we are getting constant outlet air temperature in the comfort temperature range up to total mass of PCM is melted. Beyond this point output air temperature increases rapidly which represents that PCM temperature will also increase rapidly

mentioned here are the flow rates with single air channel *i. e.* total flow rate is five times of these values. For analysis purpose it is assumed that PCM is fully charged at its melting point and no sensible heat is considered for this analysis part only. The reason behind no sensible heat consideration is that here latent heat action is of more interest than sensible heat for this type of storage system (sensible heat is 10% of the latent heat).

Here velocity of air has been assumed to be constant as 2.5 m/s and air gap will vary according to the flow rate required. it has been ensured that for all air flow rates, the air gap re-

The length of storage unit corresponding to NTU value 5, as shown fig. 7, is the minimum length at which temperature of the air will almost become equal to the material temperature, while only latent heat of the material is being considered. Therefore increasing the length of storage unit beyond this value will have no affect on the outlet temperature of air. NTU depends upon heat transfer coefficient and the surface area of the path along which air is moving. For surface area width of the channel is kept constant while the length of the air channel can be increased or decreased. So according to figs. 4 and 7 higher air flow rates will require much larger storage length to exchange heat with PCM to be in comfort tem-

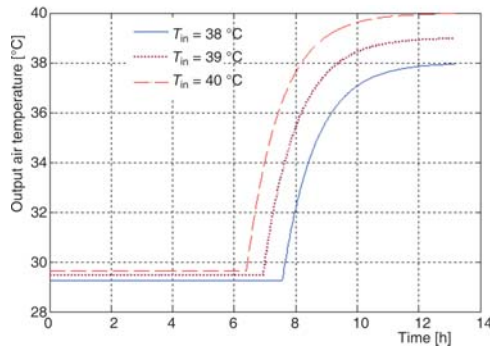


Figure 8. Output air temperature against operating time for different inlet air conditions during day time operation, $M_{PCM} = 15\text{ kg}$, $l = 2.0\text{ m}$, $\dot{V} = 40\text{ m}^3/\text{h}$

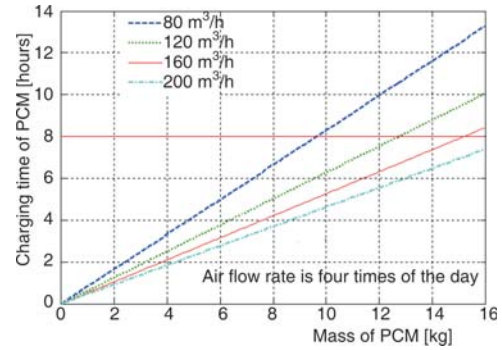


Figure 9. Charging time of storage unit against mass of PCM for different air flow rates $l = 2.0\text{ m}$, $T_{in} = 24\text{ °C}$

because sensible heat is very less as compare to latent heat due to very low specific heat of PCM. Increased inlet air temperature will always provide less time of comfort temperature as compare to decreased inlet air temperature. Change in inlet air temperature do not have effect on discharge time of storage unit, it is approximately 12 hours for all inlet air temperatures.

Figure 9 shows the effect of limited summer night time on charging of PCM for different air flow rates. If 15 kg of mass is considered for solidification during night time it can be totally solidified in 8 hours for the storage unit length of 2.0 m with the air flow rate of 160 m³/h which four times of 40 m³/h, while the same mass can provide comfort temperature for about 8 hours with 2 meters plate length.

Charging time required for PCM is most important parameter to be analyzed during this study due to limited time and temperature availability during night in summer season. In fig. 10 three different possible ambient temperatures during summer night are considered which are 23 °C, 24 °C, and 25 °C and air flow rate is four times as compare to day time air flow rate of 40 m³/h. As the ambient temperature available during night increases the time required for charging also increases. According to fig. 10, 15 kg mass of PCM per channel will require eight hours at inlet temperature of 24 °C.

Figure 11 shows the outlet air temperature for different types of artificial roughness on the air duct. The artificial roughness wedge shaped ribs, circular ribs, V shaped ribs and expanded metal mesh and chamfered rib-groove require only 2.4 m, 2.3 m, 2.0 m, 1.75 m, and 1.5 m length of storage unit, respectively, for 30 °C outlet air temperature in comparison to 3.75 m length required for smooth surface. Figure 12 shows that expanded metal mesh is having maximum Δp but V shaped ribs and chamfered rib-groove are having almost same Δp . According to figs. 11, 12 the chamfered rib-groove roughness is the best option to reduce the length of storage unit.

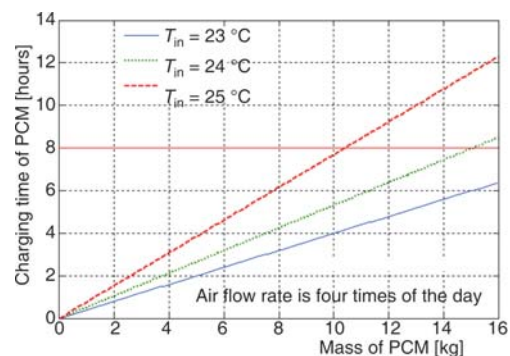


Figure 10. Charging time against mass of PCM for different inlet air temperature $l = 2.5\text{ m}$, $\dot{V} = 160\text{ m}^3/\text{h}$

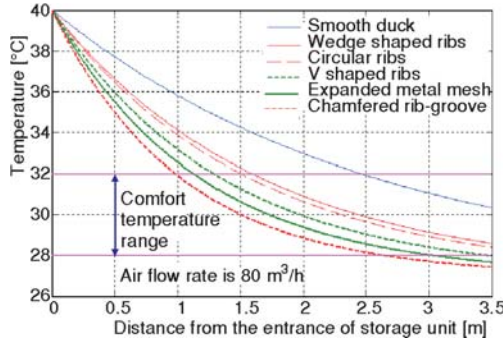


Figure 11. Outlet air temperature vs. length of storage unit for various types of artificial roughness (during day time operation) $\dot{V} = 80 \text{ m}^3/\text{h}$ $T_{in} = 40^\circ\text{C}$

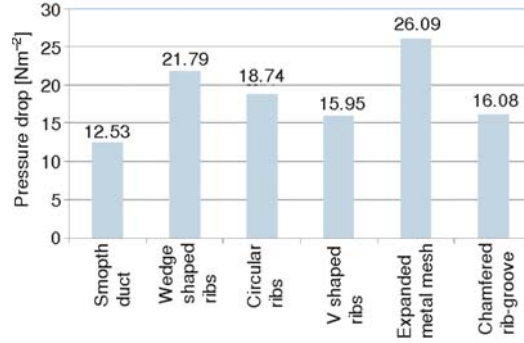


Figure 12. Pressure drop across the duct vs. types of artificial roughness, $\dot{V} = 80 \text{ m}^3/\text{h}$

Conclusions

Storage of the night coolness in the climatic conditions where summer is very harsh is a challenging work but it is possible by use of PCM for obtaining comfort temperature air during day time. Mass of PCM and air flow rate plays vital role in obtaining the comfort temperatures to certain period of time during the day operation but during night time operation air flow rate and night ambient temperature plays vital role and these will decide how much mass of PCM can be solidified in limited summer time of eight hours. It has been found that four times of air flow rate will be required as compare to required air flow rate during the day time so that it can be charged in limited night time of eight hours and it can provide comfort temperature for about eight hours during day time. Increase in the NTU value beyond five (*i. e.* increase in the length of storage unit) has no significance because it will not affect the exit air temperature for latent heat utilization. Use of artificial roughness effectively reduces the length of storage unit. Amongst all the artificial roughness used for the analysis the chamfered rib-groove is providing minimum Δp and the length of storage unit required is also minimum.

Nomenclature

A_c	– cross-sectional area of air channel, $[\text{m}^2]$
A_s	– surface area of heat exchanging plate, $[\text{m}^2]$
a	– air gap, $[\text{m}]$
b	– width of storage unit, $[\text{m}]$
$C_{p,a}$	– specific heat of air, $[\text{kJkg}^{-1}\text{K}^{-1}]$
$C_{p,pcm}$	– specific heat of PCM, $[\text{kJkg}^{-1}\text{K}^{-1}]$
D_h	– hydraulic diameter $[= 2ab/(a+b)]$, $[\text{m}]$
e	– rib height, $[\text{m}]$
e^+	– Roughness Reynolds number, $[-]$
f	– friction factor, $[-]$
h_a	– convection coefficient for air, $[\text{Wm}^{-2}\text{K}^{-1}]$
L	– length of storage unit, $[\text{m}]$
l	– latent heat of PCM, $[\text{kJkg}^{-1}]$
M_{pcm}	– mass of PCM, $[\text{kg}]$
\dot{m}_a	– mass flow rate of air, $[\text{kg}]$
NTU	– number of transfer units $(= h_a A_s / \dot{m}_a C_{p,a})$
Nu	– Nusselt number $(= h_a D_h / k_a)$, $[-]$
P	– roughness pitch, $[\text{m}]$
Δp	– pressure drop $(= 4 f l u_a^2 \rho_a / 2 D_h)$, $[\text{Nm}^{-2}]$

Re	– Reynolds number $(= \rho_a u_a D_h / \mu)$, $[-]$
r	– long way of mesh, $[\text{m}]$
s	– short way of mesh, $[-]$
T	– temperature, $^\circ\text{C}$
T_{ic}	– indoor comfort temperature, $^\circ\text{C}$
T_m	– melting point of PCM, $^\circ\text{C}$
T_{mo}	– outdoor mean temperature, $^\circ\text{C}$
T_{pcm}	– temperature of PCM, $^\circ\text{C}$
Δt	– time interval, $[\text{s}]$
u_a	– velocity of air in the channel, $[\text{ms}^{-1}]$
\dot{V}_a	– volume flow rate of air, $[\text{m}^3\text{h}^{-1}]$

Greek symbols

α_A	– angle of attack for V shaped rib, $[\text{degree}]$
α_C	– chamfer angle of rib, $[\text{degree}]$
α_R	– rib wedge angle, $[\text{degree}]$
δ	– boundary layer thickness, $[\text{m}]$

Superscript

a	– air	in	– inlet condition to storage unit
n	– previous time-step	out	– outlet condition from storage unit
$n+1$	– current time step	i	– number of node in x direction

References

- [1] Hed, G., Bellander, R., Mathematical Modelling of PCM Air Heat Exchanger, *Energy and Buildings*, 38 (2006), 2, pp. 82-89
- [2] Alkilani, M. M., *et al.*, Output Air Temperature Prediction in a Solar Air Heater Integrated with Phase Change Material, *European Journal of Scientific Research*, 27 (2009), 3, pp. 334-341
- [3] Strith, U., Butala, V., Energy Saving in Building with PCM Cold Storage, *International Journal of Energy Research*, 31 (2007), 15, pp. 1532-1544
- [4] Arkar, C., Medved, S., Free Cooling of a Building Using PCM Heat Storage Integrated into the Ventilation System, *Solar Energy*, 81 (2007), 9, pp. 1078-1087
- [5] Medved, S., Arkar, C., Correlation between the Local Climate and the Free-Cooling Potential of Latent Heat Storage, *Energy and Buildings*, 40 (2008), 4, pp. 429-437
- [6] Morrison, D. J., Abdel-Khalik, S. I., Effects of Phase-Change Energy Storage on the Performance of Air-Based and Liquid-Based Solar Heating Systems, *Solar Energy*, 20 (1978), 1, pp. 57-67
- [7] Solomon, A., Some of Approximations of Use in Predicting the Behavior of a PCM Cylinder Array, *Letters in Heat and Mass Transfer*, 8 (1981), 3, pp. 237-246
- [8] Virgone, J., *et al.*, In-situ Study of Thermal Comfort Enhancement in a Renovated Building Equipped with Phase Change Material Wallboard, *Renewable Energy*, 36 (2011), 5, pp. 1458-1462
- [9] Susman, G., *et al.*, Tests of Prototype PCM "Sails" for Office Cooling, *Applied Thermal Engineering*, 31 (2011), 5, pp. 717-726
- [10] Incropera, F. P., Dewitt, D. P., *Fundamentals of Heat and Mass Transfer*, John Wiley and Sons, New York, USA, 2008
- [11] Varun, S. M., Performance Estimation of Artificially Roughened Solar Air Heater Duct Provided with Continuous Ribs, *International Journal of Energy and Environment*, 5 (2010), 1, pp. 897-910
- [12] Nicol, F., Roaf, S., Pioneering New Indoor Temperature Standards: the Pakistan Project, *Energy and Buildings*, 23 (1996), 3, pp. 169-174
- [13] Raja, I. A., *et al.*, Thermal Comfort: Use of Controls in Naturally Ventilated Buildings, *Energy and Buildings*, 33 (2001), 3, pp. 235-244
- [14] Verma, S. K., Prasad, B. N., Investigation for the Optimal Thermohydraulic Performance of Artificially Roughened Solar Air Heaters, *Renewable Energy*, 20 (2000), 1, pp.19-36
- [15] Saini, R. P., Saini, J. S., Heat Transfer and Friction Factor Correlations for Artificially Roughened Ducts with Expanded Metal Mesh as Roughened Element, *International Journal of Heat and Mass Transfer*, 40 (1997), 4, pp. 973-986
- [16] Momin, M. E., *et al.*, Heat Transfer and Friction in Solar Air Heater Duct With V-Shaped Rib Roughness on Absorber Plate, *International Journal of Heat and Mass Transfer*, 45 (2002), 16, pp. 3383-3396
- [17] Bhagoria, J. L., *et al.*, Heat Transfer Coefficient and Friction Factor Correlations for Rectangular Solar Air Heater Duct Having Transverse Wedge Shaped Rib Roughness on the Absorber Plate, *Renewable Energy*, 25 (2002), 3, pp. 341-369
- [18] Layek, A., *et al.*, Second Law Optimization of a Solar Air Heater Having Chamfered Rib-Groove Roughness on Absorber Plate, *Renewable Energy*, 32 (2007), 12, pp. 1967-1980
- [19] Shukla, S. K., Singh, S. K., Analysis of PCM Storage Unit for Night Coolness Storage in Summer Season, *International Journal of Sustainable Energy*, 30 (2011), 2, pp.1-13